NJC

Accepted Manuscript

This article can be cited before page numbers have been issued, to do this please use: R. Mohanraj, S. Anandan and M. Ashokkumar, *New J. Chem.*, 2019, DOI: 10.1039/C9NJ01632E.

ROYAL SOCIETY OF CHEMISTRY

rsc.li/njc

Journal Name

ROYAL SOCIETY OF CHEMISTRY View Article Online
DOI: 10.1039/C9NJ01632E

ARTICLE

Luminescent On-Off Probe based Calix[4]arene Linked through Triazole with Ruthenium (II) Polypyridine Complexes to Sense Copper (II) and Sulfide ions

Received 00th January 20xx,
Accepted 00th January 20xx

DOI: 10.1039/x0xx00000x

www.rsc.org/

Mohanraj Ramachandran [a], Sambandam Anandan [*a] and Muthupandian Ashokkumar [b]

Bis-Ruthenium(II) polypyridyl complex was connected with p-tert-butyl calix[4]arene platform (**Ru_2L**) through 1,2,3-triazole and used as a luminescent probe to detect selected ions. **Ru_2L** acted as a highly sensitive and selective turn off sensor towards Cu^{2+} ion in CH_3CN/10mM HEPES buffer (pH = 7.4) (8/2, v/v) medium. The detection limit of Cu^{2+} was found to be 4.11 μM. The Cu^{2+} ion binding with **Ru_2L** showed paramagnetic signal in EPR analysis. The ensemble (**Ru_2L-Cu^{2+}**) was investigated with a variety of anions, only sulfide anion enhanced the emission intensity in the presence of other anions. The ensemble works as a turn-on sensor towards S^{2-} via metal ion displacement method to form stable CuS. The detection limit of S^{2-} was estimated from the emission intensity is to be 0.35 μM, which is an excellent result from supramolecular platform based sensors in an aqueous medium. The **Ru_2L** also showed low cytotoxicity against Human lung cancer cell lines A549 and hence can be used in cell imaging.

Introduction

Well designed judicious receptors are necessary for detecting specific ions and molecules in the area of sensors. Especially, determining the existence of metal ions and anions is of great interest in the field of chemical sensors. Copper is one of the most crucial and third abundant trace elements in the living biosystem.[1,2] Under physiological conditions, the minimum or maximum level of copper ion variation from normal level can produce dangerous biological effects.[3,4] Sensing of biologically relevant anions has been one of the most interesting fields, since monitoring its level would provide resistance to many diseases. Detection of inorganic sulfide ion (S^{2-}) in living cells is of great importance. In biological systems, sulfide anions are generated by sulfur-containing amino acids present in meat protein as well as microbial reduction of sulfate by bacteria.[5,6] The sulfide anions are extensively produced in many industrial processes and contaminate the enviroment[5]. The excess level of sulfide exposure can cause diseases like unconsciousness, paralysis, and mucosa.[7-9] There is a need to develop a sensor for the selective detection of sulfide ions.

Recently many sensors have been developed using supramolecular architectures. Calix[4]arene is a supramolecular platform. For instance, Cyclodextrin, Calixarene, Rotaxane. Calix[4]arenes are cyclic oligomers composed of phenol units associated through methylene groups, possessing specific conformational properties and cavities that are capable of encapsulating neutral and ionic species.[10-11] Calix[4]arene based sensor is used to detect the availability of cation and anion using different methods, for example, photophysical, electrochemical, nanometal, self-assembled monolayer.[11,12-14]

The photophysical method is an emerging technique for analyzing and detecting specific ions and molecules. The mechanisms involved in the photophysical method include Photoinduced Electron Transfer (PET), Photoinduced Charge Transfer (PCT), Aggregation-Induced Emission (AIE), and Forster Resonance Energy Transfer (FRET).[12,15]

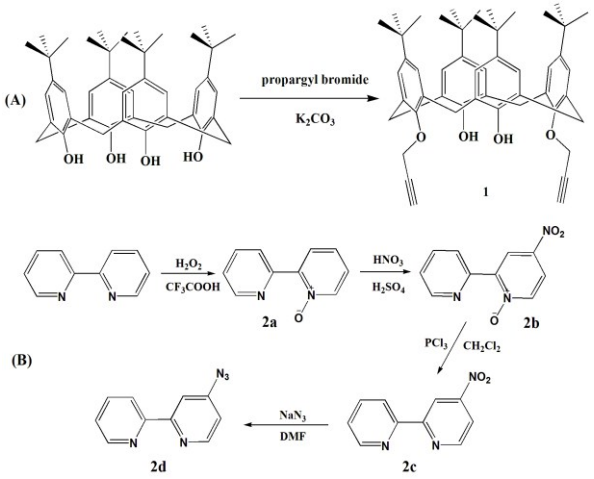

Scheme 1. (A) Synthetic route for 5,11,17,23-tetra-t-butyl-25,27-bis(O-propargyl)calix[4a]rene (**1**) and **(B)** Synthetic route for 4-azido-2,2'-bipyridyl (**2d**)

[a] *Department of Chemistry, National Institute of Technology, Tiruchirappalli-620 015, India*
[b] *School of Chemistry, University of Melbourne, Vic 3010, Australia.*
† Footnotes relating to the title and/or authors should appear here.
Electronic Supplementary Information (ESI) available: [details of any supplementary information available should be included here]. See DOI: 10.1039/x0xx00000x

View Article Online
DOI: 10.1039/C9NJ01632E

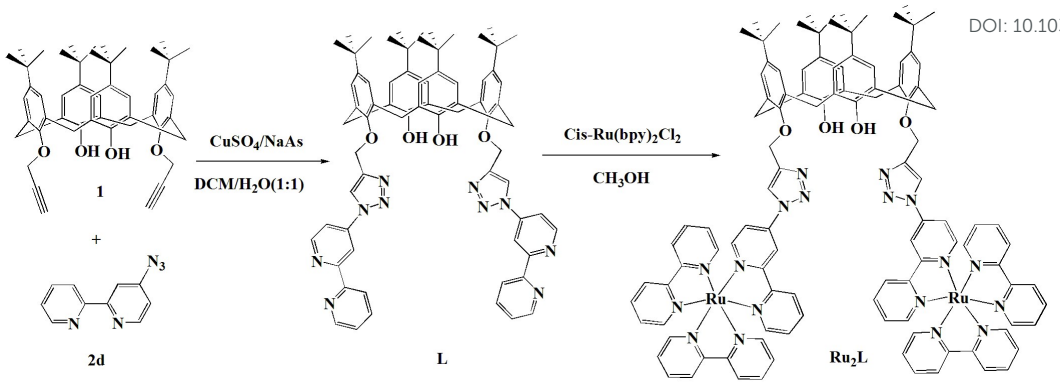

Scheme 2. Synthetic route for **L** and **Ru_2L**

As per the PET mechanism, the fluorophore provides a signal upon ion binding with the ionophore.

Many designed molecules with a variety of fluorogenic moieties such as Pyrene, BODIPY, Ru(II) complexes are used for the PET process.[16-18] Ru(II) polypyridyl complexes have been extensively accepted as a chromosphere due to their immense photochemical and electrochemical properties. Ru(II) polypyridyl complexes have been used in many applications such as DNA interaction, anticancer agent, photodynamic therapy, water oxidation catalysts and as a fluorophore in sensors.[19-22] Particularly in the growing field of anticancer activity, ruthenium-based complexes with wide stable oxidation states (II, III, and IV) under physiological condition take part as an alternative for platinum complexes.[23-28] Many toxic heavy metal ions and biologically important anions are selectively monitored by using diverse luminescent Ru(II) complexes.[29-31] Triazole, amide, and ester are different types of linkers used to connect the Ru(II) polypyridyl fluorophore with a binding core of the analyte molecule. Triazole unit has attracted much attention due to its electron rich and electron deficient nitrogens.[30,32,33] The bridging triazole, which acts as a linker in between the fluorophore and calix[4]arene, was used in sensors to sense metal ions as well as anions.[11,34-37] Various signaling units were placed in the sensory probe with triazole modified calix[4]arene.[12,38-41]

Several common types of ON-OFF, OFF-ON, ON-OFF-ON fluorescent tactics were used in sensing of ion and molecules.[42-45] Many receptors are reported based on copper-organic fluorophore ensembles[46-49], copper-nanoparticles ensembles[50,51] and a few analytes in Ru-Cu ensembles are also available.[52-54] Herein, we report on the design and application of Ru(II) polypyridyl complex (**Ru_2L**) as a luminescent probe conjugated through triazole with the help of the calix[4]arene platform. The biological activity of the developed sensor was evaluated using human lung cancer (A549) cells. The probe developed showed selectively towards Cu^{2+} ion. The emission was quenched only with that paramagnetic Cu^{2+} ion, without interference from other metal ions. **Ru_2L** luminescence could be reverted by incremental addition of sulfide anion to **Ru_2L-Cu^{2+}** ensemble. This is a novel observation to recognize sulfide anion by employing a metal displacement method, using copper coordinated triazole moiety.

Result and discussion

Synthesis and Characterization of 5,11,17,23-tetra-t-butyl-25,27-[bis(O-methyl)-2H-triazole-4-2,2'bipyridyl]calix[4]arene (L) and Bis-ruthenium polypyridyl-triazole-4-2,2'-bipyridylcalix[4]arene (Ru_2L)

The synthetic procedure of **1, 2d** and **L, Ru_2L** is shown in Scheme 1 and Scheme 2. The characterization results are included in supporting information (S1-S17). 4-azido-2,2'-bipyridine was synthesized from 4-nitro-2,2-bipyridine. Three steps were involved in synthesizing of 4-nitro-2,2'-bipyridine. Initially, selective oxidation takes place on one of the nitrogens in 2,2'-bipyridine by H_2O_2/TFA and a quantitative conversion of 2,2'-bipyridine-N-oxide was observed. When nitration takes place on 2,2'-bipyridine-N-oxide using a nitrating mixture (as fuming HNO_3/H_2SO_4), 40% yield of 4-nitro-2,2'-bipyridine-N-oxide was observed. Further 4-nitro-2,2'-bipyridine-N-oxide was reduced with phosphorous trichloride to obtain 4-nitro-2,2'-bipyridine. Using CuAAC click reaction, the ligand (**L**) was prepared (Yield 41%) from **1** and **2d** with $CuSO_4.5H_2O$ and sodium ascorbate in DCM:Water (1:1 v/v) medium. The singlet peak at 9.04 ppm and a new band at 3156 cm^{-1} are the indications for triazole formation from ^{1}H NMR and FT-IR spectra, respectively (See figure S1-S17). The complex Ru_2L was synthesized by the reaction of cis-Ru(bpy)$_2$Cl$_2$ with a corresponding amount of **L** in CH_3OH. The proton NMR spectrum of **Ru_2L** clearly shows by two peaks that calix[4]arene retained its cone conformation. The peaks appeared at 3.24, 4.09 ppm (for bridging methylene of calix[4]arene) and the peaks at 0.99, 1.34 ppm (for tert-butyl group containing hydrogen) (See figure S1-S17) also confirmed the cone conformation of calix[4]arene in the solution state.[36,55] The formation of **L** and **Ru_2L** was also confirmed by ^{1}H, ^{13}C NMR, FT-IR, Mass spectra and Elemental analysis (See figure S1-S17).

View Article Online
DOI: 10.1039/C9NJ01632F

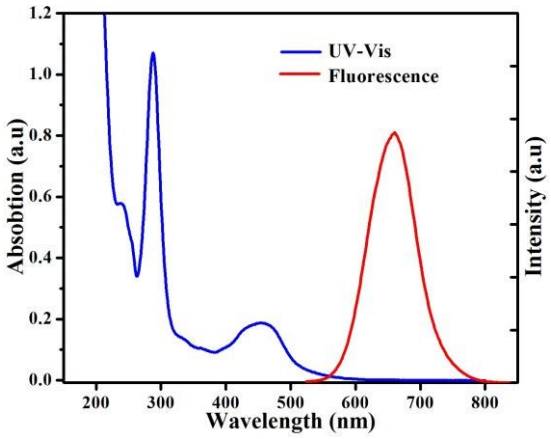

Fig.1. Combined UV-Vis and Fluorescence Spectra of **Ru_2L** (10 μM) in CH_3CN/HEPES Buffer (pH = 7.4) (8/2, v/v).

Luminescence behaviour of Ru_2L towards metal ions

UV-Vis absorption spectrum of **Ru_2L** shows three bands (Fig. 1) in CH_3CN/10 mM HEPES buffer (pH = 7.4) (8/2, v/v). Intense higher energy transitions corresponding to n-π* and π-π* bands appear at 241 and 288 nm, respectively. Another intense band appears at 457 nm from low energy singlet state metal to ligand charge transfer (^{1}MLCT). At room temperature, UV-Vis spectrum of Ru_2L was screened towards various types of metal ions: Ag^+, Al^{3+}, Fe^{2+}, Hg^{2+}, Mg^{2+}, Mn^{2+}, Na^+, Ni^{2+}, Pb^{2+} Zn^{2+}, Fe^{3+}, Ca^{2+} and Co^{2+} (10 equiv.) and Cu^{2+} (4 equiv.) in CH_3CN/10 mM HEPES buffer (pH = 7.4) (8/2, v/v) (Fig. S.18A). There is no significant difference in the UV-Vis spectra among these ions. However, a hyperchromic effect is observed upon addition of different concentrations of Cu^{2+} ion (0-4 equiv.) (Fig. S.18B). No colour change was noticed by naked eye detection while adding copper ions.

However, under UV light illumination, a red-orange luminescence of Ru_2L was turned off upon the addition of copper ions (Fig. S.19A). Upon excitation at the MLCT band region, **Ru_2L** can emit intense luminescence at 637 nm in CH_3CN/10 mM HEPES buffer (pH = 7.4) (8/2, v/v) at room temperature due to ^{3}MLCT dπ(Ru) → dπ* transition (Fig. 1). The luminescence behaviour of **Ru_2L** was examined with a wide range of metal ions (toxic metals and metals present in biological organisms) up to 10 equiv. ratio (Fig. 2A). Interestingly, the emission intensity of **Ru_2L** is significantly quenched only with 4 equiv. of Cu^{2+} ions (Fig. 2B) whereas the emission intensity is only slightly affected upon the addition of some other metal ions.[53,56] The photoelectron transfer (PET) mechanism (photoelectron transferred from excited state of Ru moiety to paramagnetic Cu^{2+} ion) was the reason for luminescence quenching.[57] Nearly 80% of luminescence intensity is quenched by Cu^{2+} ions whereas about 22-25% of the intensity was quenched by Fe^{2+} and Ni^{2+}. The binding constant value (2.31 x 10^4) was calculated from the emission spectra for **Ru_2L** interaction with copper (II) ion which is good agreement with already reported values.[53] The detection limit value is found to be 4.11 x 10^{-6} M from emission spectra, which is convincingly higher selectivity compared to the level of detection by the U.S. environmental protection agency (20 x 10^{-6} M of copper ion in drinking water).[53] Other metal ions interference of **Ru_2L-Cu^{2+}** study with copper (II) ion was carried out and its luminescence intensity can be seen from Fig. 3A that there is insignificant interference by other metal ions. A linear dependency of fluorescence intensity on Cu^{2+} ion concentration (r = 0.9948) was obtained (Fig. 3B). From these results, **Ru_2L** can be found to be a highly reliable probe for detecting Cu^{2+} ions in the presence of other cations. No significant change was noticed in the luminescence behaviour upon moving to acidic to neutral pH in the presence of Cu^{2+} ions. Whereas moving from neutral to basic pH in the presence of Cu^{2+} ions, the emission intensity was found to decrease (Fig. S.20B) probably due to the deprotonation of the two hydroxyl

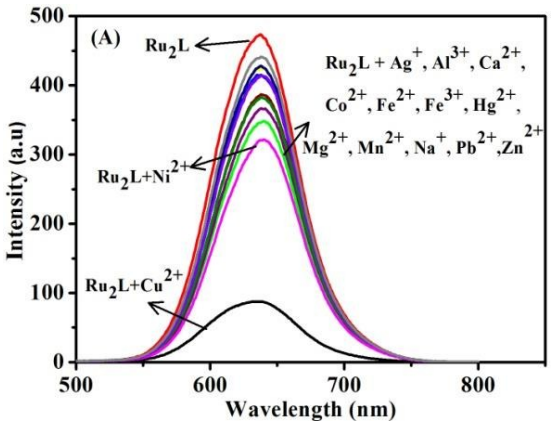

Fig.2. (A) Emission spectra of **Ru_2L** (10 μM) with various types of metal ions (10 equiv.) and Cu^{2+} ion (4 equiv.) in CH_3CN/HEPES buffer (pH = 7.4) (8/2, v/v).

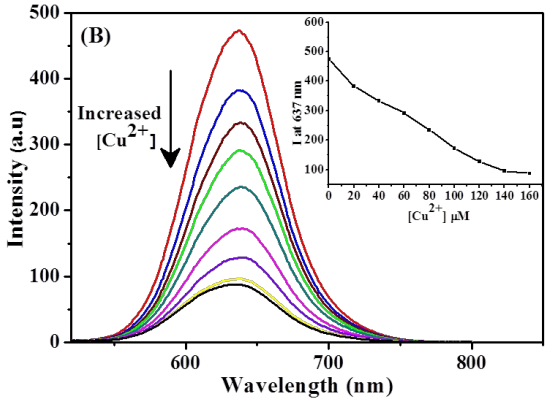

Fig.2. (B) Incremental addition of Cu^{2+} ion (0-4 equiv.) to **Ru_2L** (10 μM) in CH_3CN/HEPES buffer (pH = 7.4) (8/2, v/v).

View Article Online
DOI: 10.1039/C9NJ01632E

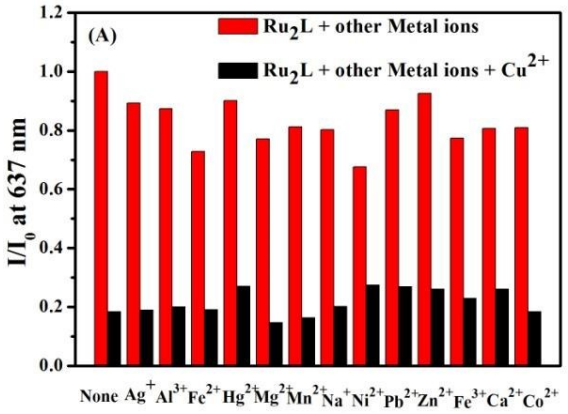

Fig.3. (A) Interference study of bar diagram of **Ru_2L+Cu^{2+}** (10 μM) with various types of metal ions (10 equiv.).

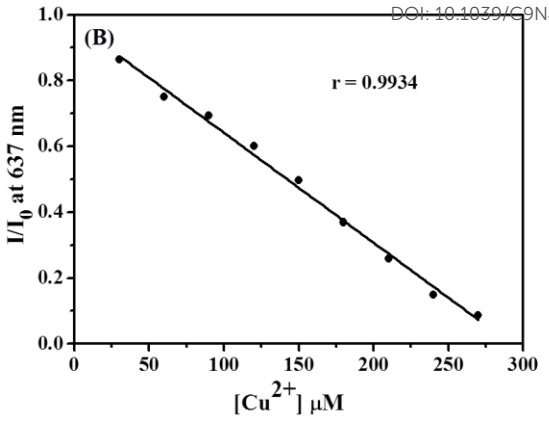

Fig.3. (B) Linear plot of incremental addition of Cu^{2+} ion to **Ru_2L** in CH_3CN/HEPES buffer (pH = 7.4) (8/2, v/v).

groups of calix[4]arene. Even at higher pH range in the absence of Cu^{2+} ions, there is no luminescent quenching because t-butyl substituent of p-tertbutyl calix[4]arne moiety can effectively perturb the formation of quinone (from phenol) moiety which is a quencher to ruthenium polypyridyl complexes.

EPR and Electrochemical studies

To further confirm the copper ion binding, EPR measurements were made. The spectra were recorded with a microwave frequency of 9.8 GHz in CH_3CN at room temperature and liquid nitrogen temperature. At room temperature, there is no EPR signal for **Ru_2L** due to the diamagnetic character of Ru^{2+} ions. Addition of Cu^{2+} ions to **Ru_2L** a new signal around 312 mT which corresponds to the binding of Cu^{2+} ion on **Ru_2L** (**Ru_2L-Cu^{2+})** (Fig. S.21A) was observed. The hyperfine splitting pattern (peak at 2.34 and 2.04 responded to average $g_{\parallel}$ and $g_{\perp}$ values, respectively) was observed clearly at liquid nitrogen temperature (Fig. S.21B). From the above findings, it is observed that $g_{\parallel} > g_{\perp} > 2.003$ for **Ru_2L-Cu^{2+}** which illustrate the characteristic of d_9 copper (II) and a ground state doublet representing the existence of an unpaired electron in the $d_{x^2-y^2}$ orbitals.[57,58]

The electrochemical properties of **Ru_2L** and **Ru_2L-Cu^{2+}** were studied using three electrode cyclic voltammetric system in degassed and dry CH_3CN solvent with tetrabutylammonium hexafluorophosphate as supporting electrolyte (Fig. S.22A). $[Ru(bpy)_3]^{2+}$ was taken as a reference complex, which generates one positive potential from Ru^{II}/Ru^{III} redox process and three negative potentials from bipyridine moiety.[59] **Ru_2L** exhibits two reversible oxidation potentials and one quasi-reversible process occurring at +1.08 V vs Ag/AgCl which is responsible from Ru^{III}/Ru^{II} process of dinuclear ruthenium complexes. The peak value of dinuclear ruthenium complex was shifted towards negative side compared to mononuclear ruthenium complex due to two one-electron Ru^{III}/Ru^{II} redox process, but only one oxidation potential is obtained for dinuclear ruthenium complex.[31] The second reversible potential was obtained at +0.76 V, due to the tertiary amine oxidation process. The **Ru_2L-Cu^{2+}** exhibits three reversible oxidation potentials at +1.17, +0.76 and +0.47 V in the particular window range (-0.5 to 1.6 V). First, two potentials were assigned to Ru^{III}/Ru^{II} redox process, a tertiary amine oxidation process and the third one +0.47 V was assigned to the copper ion (Cu^{II}/Cu^{I} vs NHE) redox potential process.[60] The luminescent lifetime decay profile diagram of **Ru_2L** and the ensemble (**Ru_2L-Cu^{2+}**) shows a bi-exponential decay and were represented in Fig. S.22B. In the absence of copper (II) ion, **Ru_2L** shows a bi-exponential decay with lifetime τ_2 = 38 ns at room temperature. The lifetime of **Ru_2L-Cu^{2+}** ensemble was decreased by twenty nanoseconds (from τ_2 = 38 to 18 ns) when compared to **Ru_2L**. A small lifetime change is attributed to the decay of the excited state quenched by photoinduced electron transfer (PET).[60]

Luminescence behaviour of Ru_2L-Cu^{2+} towards anions

The ensemble (**Ru_2L-Cu^{2+}**) contains supramolecular platform, it could be formed 1:1 ratio from Ru_2L and Cu^{2+} ion in CH_3CN/10mM HEPES buffer (pH = 7.4) (8/2, v/v). Only negligible changes occurred in absorption spectra of the ensemble with sulfide anion (7 equiv.) whereas no changes were observed even the addition of 10 equiv. of various kind of anions like CH_3COO^-, CN^-, CO_3^{2-}, Cys, F^-, HPO_4^-, HSO_4^-, NO_2^-, NO_3^-, ^-OH, SO_3^{2-} and GSH in CH_3CN/10mM HEPES buffer (pH = 7.4) (8/2, v/v). The luminescence behaviour of Ru_2L-Cu^{2+} was checked with 10 equiv. of above mentioned various anions in CH_3CN/10mM HEPES Buffer (pH = 7.4) (8/2, v/v) (Fig. 4A). From these scanning results, it can be seen that sulfide anion behaves different to other anions in enhancing the emission intensity of the ensemble. The emission intensity of the ensemble was increased gradually at 637 nm upon addition of 0-7 equiv. of S^{2-} anion (Fig. 4B). This is caused by the formation of stable copper sulfide or the development of Cu_xS_x rings in solution.[61] Sulfur ion has more affinity towards Cu^{2+} ion (compared to nitrogen and oxygen) and for this reason, its luminescence properties of **Ru_2L** is retained.

View Article Online
DOI: 10.1039/C9NJ01632E

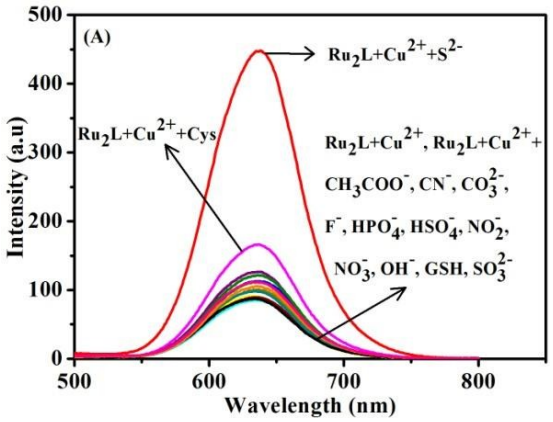

Fig.4.(A) Emission spectra of **Ru_2L-Cu^{2+}** (10 μM) with different types of anions (10 equiv.) and S^{2-} anion (7 equiv.)

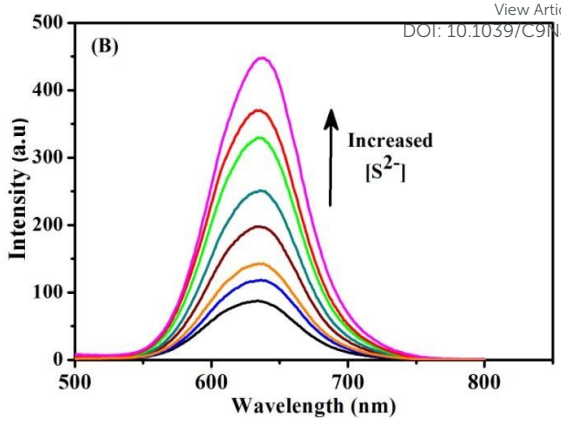

Fig. 4.(B) Incremental addition of S^{2-} anion (0-7 equiv.) to **Ru_2L-Cu^{2+}** in CH_3CN/HEPES buffer (pH = 7.4) (8/2, v/v).

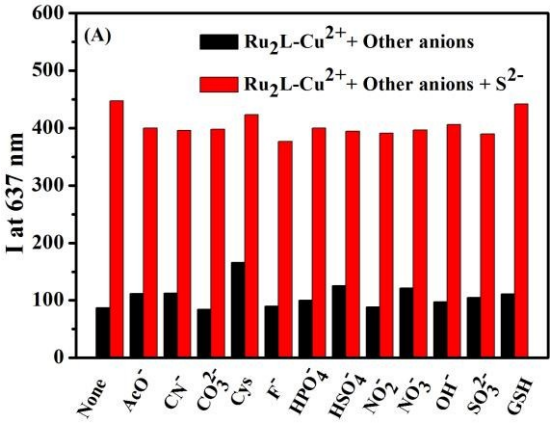

Fig.5.(A) Interference study from the emission spectra of **Ru_2L-Cu^{2+}+S^{2-}** with different types of anions (10 equiv.).

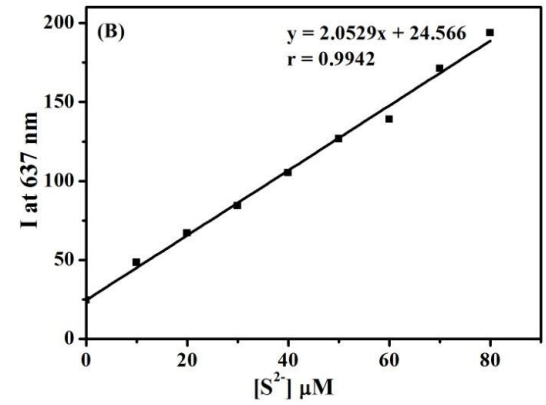

Fig.5.(B) Linear plot from incremental addition of S^{2-} ion to **Ru_2L-Cu^{2+}** in CH_3CN/HEPES buffer (pH = 7.4) (8/2, v/v).

In naked eye view, luminescence behaviour of the ensemble was investigated with all anions under UV-light illumination. Only sulfide anion responded by showing the emission enhancement (Fig. S.19B). The reason may be that the sulfide anion act as a turn-on sensor (as restored the emission intensity of **Ru_2L**) from turn-off (**Ru_2L-Cu^{2+}**). The maximum emission intensity from the ensemble was retained (98%) when S^{2-} anion was added. Interference of sulfide anion was tested in the presence of other anions with **Ru_2L-Cu^{2+}**, and in this competitive experiment, sulfide anion showed selectivity towards copper ion in the presence other anions (Fig.5A). A good linear relationship (r = 0.9918) was obtained while incremental addition of sulfide anion to **Ru_2L-Cu^{2+}** (Fig.5B). The detection limit of S^{2-} was estimated from the emission intensity of **Ru_2L-Cu^{2+}** is to be 3.56 x 10^{-7} M and it is the better result from supramolecular platform based-probe in aqueous condition.[43] Furthermore, the selectivity of the ensemble was examined with sulfide anions in variant pH level. Negligible changes were observed (Fig. S.20A). From the above discussions, **Ru_2L-Cu^{2+}** is found to be an efficient turn on luminescent probe towards sulfide anion in the presence of other anions.

Proposed Sensing Mechanism

The target complex (**Ru_2L**) is soluble in aqueous medium due to the presence of bis-ruthenium polypyridyl unit. The p-tertbutyl calix[4]arene has been found to be a successful supramolecular platform due to the formation of cone conformation modified with bis-ruthenium polypyridyl complex through triazole linker. Two hydroxyl groups would marginally assist triazole moiety for coordination with a metal ion and also render the varaible luminescent behaviour of Ru_2L. Triazole moiety acts as an excellent linker and bind efficiently with metal ions through due to the presence of other atoms capable of coordinating. The cavity of calix[4]arene, conformation of the platform, N_2O_2 (two nitrogen from triazole moiety and two oxygen from calix[4]arene) binding core and bis-ruthenium polypyridyl complex take part a major role in sensing Cu^{2+} ions and anions by fluorescence. **Ru_2L-Cu^{2+}** ensemble has a very low (5.6 fold less) luminescence compared to Ru_2L, while Cu^{2+} ion could be binding with N_2O_2 core of the probe. The binding ratio (1:1) of metal with the probe was confirmed by job plot (Fig. S23A).

View Article Online
DOI: 10.1039/C9NJ01632E

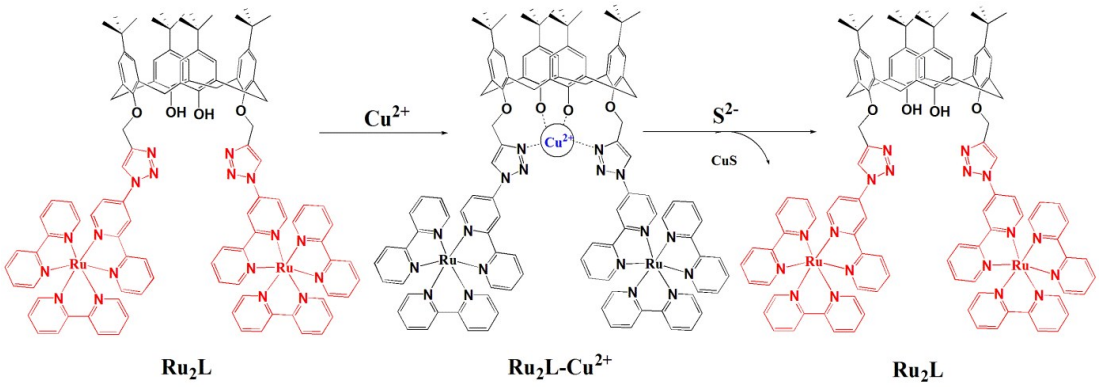

Fig.6. Proposed mechanism for Cu^{2+} ion binding with **Ru_2L** and S^{2-} anion releases Cu^{2+} ion from **Ru_2L-Cu^{2+}**.

The metal ion exchange experiment was carried out using three different pH, this result reveals that some negligible changes were obtained (Fig. S25). Using the emission intensities and the molar extinction coefficients at 457 nm, we have calculated the quantum yields of Ru_2L is 0.033 whereas quantum yields is 0.062 upon using the standard $[Ru(bpy)_3]^{2+}$. However, upon addition of Cu^{2+} ion to Ru_2L, the quantum yield was decreased from 0.033 to 0.010 whereas the quantum yield was retained back to 0.031 for the $Ru_2L+Cu^{2+}+S^{2-}$ (i.e., the addition of S^{2-}.[54]

Metal displacement approach is one of the tactics in luminescent anion sensors. In this approach, a specific anion displaces the metal ion selectively at optimum condition. The sulfide anion reacts with the ensemble to enhance luminescence due to metal displacement method (Fig. 6). The emission intensity of **Ru_2L** was retained at 98% from ensemble by metal displacement method through sulfur anion (Fig. S23B). Moreover, the sulfur ion has more coordinating power (compared to nitrogen and oxygen) towards copper (II) ion to generate copper sulfide and to enhance fluorescence by thus reformed **Ru_2L** molecule.

Cytotoxicity, AO/EB staining and Hoechst 33528 staining studies towards Ru_2L

Few ruthenium compounds have worked as a potential anticancer activity in clinical trials.[25,26] However, there are some disadvantages such as uncontrolled reactions with proteins, high cytotoxicity, and poor water solubility. MTT assay method was used to examine the cytotoxicity of **Ru_2L** against human lung cancer (A549) cell lines. Inhibition of cellular viability was tested after 24 h incubation with different concentration of the complexes (**Ru_2L**). As a result, the inhibition level increased gradually from 0 to 88% when increasing the concentration of the complex from 0 to 200 μg/ml (Fig. S26). **Ru_2L** (IC_{50} = 106.5 ± 0.5 μM) showed low toxicity towards A549 cell lines compared to cis-platin (IC_{50} = 18.5 ± 1.4 μM). Apoptosis is the process of linking a series of biochemical actions important to characteristic cell morphology modification and finally controlled cell death. The necrosis is another form of uncontrolled cell death (autolysis) divergent from apoptosis where uncontrolled cell death leads to lysis of cells.[62] Initially, A549 cell lines were incubated with **Ru_2L** for 24 h. After that, the treated cell lines were stained

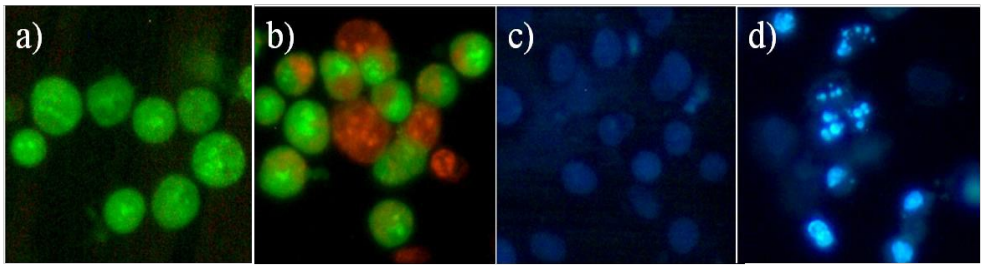

Fig.7. AO/EB staining of A549 cells with the control (a), incubated with **Ru_2L** complex (b) showing the variations in nuclear morphology and Hoechst 33258 staining of A549 cells with the control (c), treated with **Ru_2L** complex (d) screening the changes in nuclear morphology.

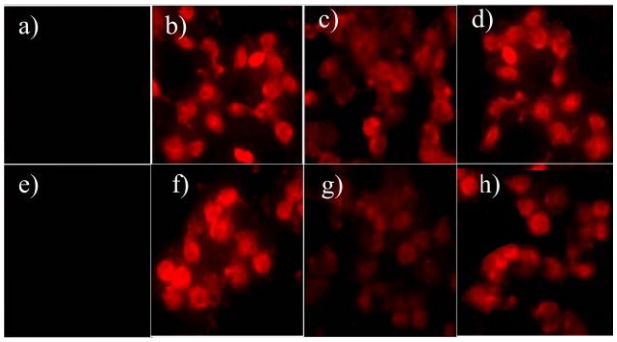

Fig.8. The controlled A549 cells (a and e) treated with **Ru_2L** (10 μM) for 1 h (b and f) and the cells were incubated with two different concentration of Cu^{2+} ion such as 10 μM (c), 20 μM (g) for 60 min and then **Ru_2L-Cu^{2+}** loaded cells were further treated with two different concentration of sulfide anion 20 μM (d) and 40 μM (h).

with acridine orange (AO) and ethidium bromide (EB) solution. Morphological changes at the time of cell death are significant criteria in apoptosis that can be studied via AO/EB staining. The control or viable cells became visibly green having uniform chromatin with the inviolate cell membrane. Early apoptotic features such as cell shrinkage, condensation, fragmentation were spotted mostly in **Ru_2L** treated cells. Further, a small fraction of cells show the morphology of blebbing, apoptotic bodies and a very few necrosis modes of cell death also appeared in orange-red colour (Fig. 7). Human lung cancer cell lines were incubated with IC_{50} dose of the method and monitoring the changes in cytology of the cells (with special reference to the nuclei and cytoplasm). It is observed that the initial apoptotic characteristics such as cell shrinkage, chromatin condensation and fragmentation have been mostly were also noticed. The Hoechst 33528 staining (Fig. S27B) illustrates the different percentage of normal and abnormal cells from control and **Ru_2L** treated cells. Hence, the findings from AO/EB staining agreed with Hoechst staining results, which induce apoptosis (cell death in A549 cell lines) by the complex (**Ru_2L**).

Live cell Imaging studies

The cellular uptake was measured in terms of intracellular fluorescence intensity displayed by the treatment of **Ru_2L** with live cells. The **Ru_2L** (10 μM) treated with A549 cell lines for 1h described their localization. It is clear from the images that, **Ru_2L** is mainly present on the cytoplasm of the cells and some of them are even accumulated in the nucleus membrane. Subsequently, the Ru_2L-loaded cells were further treated with two different (10 μM, 20 μM) concentrations of Cu^{2+} for another 60 min at room temperature. **Ru_2L** complex loaded cells contain bright intracellular red luminescent, which clearly illustrates that while increasing Cu^{2+} ion concentrations, the red luminescent gradually weaken. Ru_2L-Cu^{2+} loaded cells were incubated furthermore for one hour with two different sulfide anion concentrations (20 and 40 μM) and recorded the images. It is seen that the maximum bright intracellular red luminescent was retained upon addition of S^{2-} (Fig. 8). Further studies are required to understand the interaction of **Ru_2L** with cellular organelles.

View Article Online
DOI: 10.1039/C9NJ01673E

Conclusions

Supramolecular based **Ru_2L** has been synthesized and converted to an aqueous soluble probe using hydrophobic p-tertbutyl calix[4]arene and bis-ruthenium polypyridyl complexes through triazole linker. In the presence of a wide range of metal ions, the emission intensity of **Ru_2L** was marginally quenched only with paramagnetic Cu^{2+} ion, due to photoinduced electron transfer mechanism. The binding mode 1:1 was further confirmed by the Job's plot and the binding constant was estimated to be 2.31 x 10^4 M^{-1} from the emission spectra. Upon the addition of sulfide anions to **Ru_2L-Cu^{2+}**, the weak luminescence of **Ru_2L-Cu^{2+}** significantly enhanced showing the 'turn-on' sensitivity. Thus, **Ru_2L-Cu^{2+}** could be an excellent turn-on luminescent sensor towards discriminating sulfide anions in the presence of other anions. From biological studies, **Ru_2L** complexes showed low toxicity against A549 cell lines compared to cis-platin and ruthenium polypyridine based complexes reported in the literature. Furthermore, **Ru_2L** complexes have been used in fluorescence imaging studies where it clearly differentiates the apoptosis and necrosis cells from control cells using cellular uptake, AO/EB staining and Hoechst 33528 staining methods.

Experimental Section

All synthetic procedures were carried out under an inert atmosphere. cis-$Ru(bpy)_2Cl_2$ was prepared according to the literature.[63] All chemicals were, from Alfa Aesar and Sigma Aldrich and used without further purification. The solvents CH_3CN and CH_3OH were used after distillation. Metal perchlorate salts procured from Merck were used as the source for metal ions and all anions used were tertbutyl ammonium (TBA) salts. UV-Vis and fluorescence spectra were recorded on a Specord S 600 diode-array UV-Vis spectrophotometer and Shimadzu RF-5301 PC spectrofluorophotometer, respectively at room temperature. The FT-IR spectra were recorded on a Thermo Scientific Nicolet iS5 FT IR spectrometer. The cyclic voltammetric analysis was performed on a Autolab three electrode system, where Ag/AgCl as a reference electrode, glassy carbon as a working electrode and platinum wire as a counter electrode in an acetonitrile solvent containing 0.1 M tetrabutylammonium hexafluorophosphate ($^tBu_4N^+PF_6^-$) as the supporting electrolyte with 100 mV scan rate and the system was calibrated using ferrocene/ferrocenium ion (Fc/Fc^+) standard. The matrix-assisted laser desorption/ionization-time of flight (MALDI-TOF) mass spectrometry was used to determine the mass of the sample. ^1H and ^{13}C NMR spectra were recorded with Bruker Avance 500 and AMX 400 spectrometers using $CDCl_3$ and DMSO-d_6 solvent (TMS as internal standard) in the ppm range. The luminescence lifetime

View Article Online DOI: 10.1039/C9NJ01637F

was carried out with the Time-Correlated Single Photon Counting method (TC-SPC) in a Horiba FluoroMax-4 instrument. EPR were recorded using Bruker EMX Plus X-band (9.8 GHz) spectrometer.

5,11,17,23-tetra-t-butyl-25,27-bis(O-propargyl)calix[4]arene (1)[64]

p-tert-butylcalix[4]arene (10.0 g, 15.43 mmol, 1 eq.) in dry acetone (200 mL) was stirred with potassium carbonate (5.10 g, 36.72 mmol, 2.37 eq.) at room temperature for 1 h. A solution of propargyl bromide (6.49 g, 30.86 mmol, 2 eq.) in dry acetone (50 mL) was added dropwise into the above-stirred mixture over a period of 30 min. The reaction mixture was refluxed for 24 h and was then allowed to cool to room temperature. Using a celite pad, the reaction mixture was filtered to remove insoluble particles, and the filtrate was concentrated by a rotatory evaporator. 100 mL of 2 M HCl was added to the concentrated reaction mixture, and the product was extracted with dichloromethane (3 × 100 mL). The combined organic extract was consecutively washed with water and brine (100 mL), dried over anhydrous Na_2SO_4, filtered and evaporated to dryness in a vacuum. The crude product was recrystallized from DCM/Methanol to afford 1 as a white solid (9.10 g, 82% yield). ^{1}H NMR ($CDCl_3$) δ (ppm): 7.07 (s, 4H), 6.72 (s, 4H), 6.47 (s, 2H, OH), 4.75 (d, J = 2.4 Hz, 4H), 4.37 (d, J = 13.4 Hz, 4H), 3.33 (d, J = 13.4 Hz, 4H), 2.53 (t, J = 2.4 Hz, 2H), 1.30(s, 18H), 0.89 (s, 18H). ^{13}C NMR ($CDCl_3$, 100 MHz) δ (ppm): 150.2, 149.4, 147.4, 141.7, 132.7, 128.0, 125.5, 125.0, 78.7, 63.2, 33.9, 33.8, 32.0, 31.6, 30.9. FT-IR: 2959, 2120 cm^{-1}.

2,2'-Bipyridine-N-oxide (2a)[65]

The mixture of 2,2'-bipyridine (7.8 g, 0.05 mol, 1.0 eq.) and 30% hydrogen peroxide (8.5 mL, 2.6 g, 0.075 mol, 1.5 eq.) were stirred for 6 hours in trifluoroacetic acid (40 mL) at room temperature. After that, neutralised using aqueous 6N NaOH and extracted with chloroform (4 × 50 mL). The combined organic layers were washed with aqueous saturated sodium chloride, dried over Na_2SO_4, filtered and concentrated to afford colourless oil, which solidified under vacuum into a white solid. (7.57 g, 0.044 mol, 88 %). ^{1}H NMR ($CDCl_3$) δ (ppm): 8.88 (ddd, J = 8.1,1.0 & 0.7, Hz 1H), 8.70 (ddd, J = 4.8, 1.7 & 0.9 Hz 1H), 8.30 (dd, J = 6.4 & 1.1 Hz, 1H), 8.11 (dd, J = 7.8 & 2.4 Hz, 1H), 7.80 (ddd, J = 8.0, 7.2 & 1.6 Hz, 1H), 7.34 (ddd, J = 8.0 , 7.2 & 1.2 Hz, 1H), 7.32 (ddd, J = 7.5 , 5.0 & 0.8 Hz, 1H), 7.25 (ddd, J = 7.5 , 4.0 & 2.2 Hz, 1H). (^{13}C NMR, 100 MHz) δ (ppm): 149.4, 149.2, 147.0, 140.0, 136.1, 127.6, 125.8, 125.3, 125.2, 124.1.

4'-Nitro-2,2'-bipyridine-N-oxide (2b)[65]

In an ice bath, 2,2'-Bipyridine-N-oxide (3.0 g, 17.0 mmol, 1 eq.) was dissolved in concentrated sulphuric acid (19 mL, 34.2 g, 0.349 mol, 20 eq.) under vigorous stirring. A mixture of fuming nitric acid (30 mL, 43.9 g, 0.697 mol, 40 eq.) in concentrated sulphuric acid (14 mL, 25.7 g, 0.262 mol, 15 eq.) was added dropwise over 15 min and then the reaction mixture was heated at 110°C for 5 hours. Once cooled, the solution was poured into ice (150 g) and adjusted to pH 8 using 38% aqueous NaOH. The light yellow precipitate was filtered and washed with water. The solid was dissolved in methylene chloride, the mixture was extensively extracted with water and the combined organic layers were dried over sodium sulfate, filtered and concentrated to yield 1.52 g (7.0 mmol, 40%) of 4'-nitro-2,2'-bipyridine-N-oxide as a beige solid. ^{1}H NMR ($CDCl_3$) δ (ppm): 9.16 (d, J = 3.4 Hz, 1H), 8.89 (dt, J = 8.1 & 0.8 Hz, 1H), 8.79 (ddd, J = 4.8 & 0.9 Hz, 1H), 8.36 (d, J = 7.3 Hz, 1H), 8.06 (dd, J = 7.3 & 3.3 Hz, 1H), 7.88 (td, J = 7.8 & 1.7 Hz, 1H), 7.43 (ddd, J = 6.2, 4.8 & 1.22 Hz,1H). (^{13}C NMR, 100 MHz) δ (ppm): 149.8, 148.2, 147.5, 142.4, 141.9, 136.6, 125.3, 125.0, 122.5, 118.8.

4-Nitro-2,2'-bipyridyl (2c)[65]

In an ice cooled condition, phosphorous trichloride (3.6 ml, 41.1 mmol, 3 eq.) was added to 4-nitro-2,2'-bipyridyl-N-oxide (2b) (3.00 g, 13.6 mmol, 1 eq.) in dry DCM (30 ml) and the mixture was heated at reflux for overnight. After cooling the reaction mixture was carefully poured into crushed ice and basified with 38% sodium hydroxide. The aqueous layer was exhaustively extracted with dichloromethane and the combined organic solutions were washed with water, then dried over sodium sulfate and concentrated to yield a pale yellow solid. (2.21 g, 80 %) ^{1}H NMR ($CDCl_3$) δ (ppm): 9.18 (d, J = 2.2 Hz, 1H), 8.97 (d, J = 5.3 Hz, 1H), 8.77 (d, J = 4.3 Hz, 1H), 8.49 (dt, J = 8.0 & 0.9 Hz, 1H), 8.04 (dd, J = 5.4 & 2.2 Hz, 1H), 7.90 (td, J = 7.6 & 1.8 Hz, 1H), 7.43 (ddd, J = 6.2, 4.9 & 1.2 Hz, 1H). (^{13}C NMR, 100 MHz) δ (ppm): 159.4, 155.0, 153.9, 151.2, 149.5, 137.8, 124.9, 121.4, 115.7, 113.7.

4-azido-2,2'-bipyridyl (2d)[66]

4-nitro-2,2'-bipyridyl (0.57 g, 0.4 mmol, 1 eq.) with NaN_3 (1.50 g, 3.85 mmol, 8.95 eq.) was heated in DMF (10 mL) for 5 hours at 100 °C. The solvent was removed under vacuum and water (40 mL) was added to the yellow solid, the aqueous phase was extracted with dichloromethane. The combined organic phase was dried over anhydrous sodium sulphate. The crude product was purified by flash silica column chromatography using dichloromethane/ethyl acetate (1:1) mixture. The yellow colour solid was obtained as 4-azido-2,2'-bipyridyl (yield, 0.52g, 93.54 %). ^{1}H NMR ($CDCl_3$) δ (ppm): 8.69 (ddd, J = 4.8, 1.8 & 0.9 Hz, 1H, H-6'), 8.58 (d, J = 5.4 Hz, 1H, H-6), 8.40 (dt, J = 7.8 & 0.9 Hz, 1H, H-4'), 8.15 (d, J = 2.3 Hz, 1H, H-3), 7.82 (td, J = 7.8 & 1.8, 1H, H-5'), 7.34 (ddd, J = 7.5, 4.8 & 1.2, 1H, H-3'), 6.93 (dd, J = 5.4 & 2.3 Hz, 1H, H-5). (^{13}C NMR, 100 MHz) δ (ppm): 162.5, 149.4, 148.8, 141.8, 138.4, 136.4, 125.6, 124.7, 117.5, 116.1. FT-IR (ATR): 2115 cm^{-1} (s).

5,11,17,23-tetra-t-butyl-25,27-[bis(O-methyl)-2H-triazole-4-2,2'-bipyridyl]calix[4]arene (L)

5,11,17,23-tetra-t-butyl-25,27-bis(O-propargyl)calix[4]arene **1** (0.435 g, 0.6 mmol, 1 eq.) was added to the solution of 4-

azido-2,2'-bipyridyl **2d** (0.236 g, 1.2 mmol, 2 eq.) in 30 mL of dichloromethane and water (50:50) mixture. To this solution, $CuSO_4 \cdot 5H_2O$ (15 mg, 0.06 mmol, 0.1 eq.) and sodium ascorbate (23 mg, 0.12 mmol, 0.2 eq.) were added. The resulting solution was stirred for 12 h at room temperature. Upon completion of the reaction as confirmed by TLC, the organic layer was separated and the aqueous layer was extracted with dichloromethane (2 × 25 mL). The combined organic layer was washed with water and then with brine (2 × 50 mL). The organic layer was stirred for two hours with aqueous EDTA solution and then organic layer was separated dried over anhydrous sodium sulphate, and the solvent was removed under vacuum. The crude product was purified by column chromatography using hexane: ethyl acetate (7:3) to afford white precipitate (L). Yield: 0.281 g (41%). ^{1}H NMR ($CDCl_3$): δ = 9.14 (d, 2H), 9.04 (s, 2H), 8.76 (d, 2H), 8.37 (dd, 2H), 8.32 (d, 2H), 7.89 (ddd, 2H), 7.82 (s, 2H), 7.64 (dd, 2H), 7.41 (ddd, 2H), 7.11 (s, 4H), 6.9 (s, 4H), 5.19 (s, 4H), 4.33 (d, 4H), 3.43 (d, 4H), 1.20 (s, 18H), 1.04 (s, 18H). ^{13}C NMR ($CDCl_3$); δ = 158.2, 154.8, 150.8, 150.3, 149.2, 148.0, 146.5, 143.0, 142.5, 137.0, 132.7, 127.8, 125.9, 125.4, 124.4, 121.5, 120.2, 112.4, 108.8, 70.7, 34.1, 33.9, 31.6, and 31.0. MALDI-TOF-Ms Calculated for $C_{70}H_{74}N_{10}O_4$ ($[M+Na]^+$) 1142.4; found, 1142.50. Anal. calcd for $C_{70}H_{74}N_{10}O_4$: C, 75.11; H, 6.66; N, 12.51%. Found: 75.32; H, 6.81; N, 13.06%.

Bis-rutheniumpolypyridyl-triazole-4-2,2'-bipyridylcalix[4]arene (Ru_2L)

In argon atmosphere, cis-Ru(bpy)2Cl2 (135 mg, 0.28 mmol, 2 eq.) and silver nitrate (95 mg, 0.56 mmol, 4 eq.) were stirred for 3 hours in methanol (25 mL) under room temperature. The suspension was filtered in order to remove the silver salt, and the filtrate was added to 5,11,17,23-tetra-t-butyl-25,27-[bis(O-methyl)-2H-triazole-4-2,2' bipyridyl]calix[4]arene **L** (159 mg, 0.14 mmol, 1 eq.) in methanol. The mixture was heated at reflux condition in an argon atmosphere under dark for overnight. The reaction mixture was allowed to reach room temperature and the solvent was evaporated. The remaining solid was re-dissolved in a minimum amount of methanol, and the desired compound was precipitated by the dropwise addition of a saturated aqueous solution of ammonium hexafluorophosphate. The precipitate was filtered and dried under vacuum to yield 224 mg (82 %) of the desired ruthenium complex **Ru_2L** as a red solid. ^{1}H NMR (DMSO-d_6): δ = 9.30 (d, 2H), 9.27 (s, 2H), 9.00 (d, 2H), 8.83 (m, 8H), 8.23-8.16 (m, 14H), 7.89 (ddd, 2H), 7.82 (s, 2H), 7.64 (m, 8H) , 7.59-7.51 (m, 12H), 7.41 (ddd, 2H), 7.11 (s, 4H), 6.9 (s, 4H), 5.19 (s, 4H), 4.08 (d, 4H), 3.28 (d, 4H), 1.19 (s, 18H), 0.99 (s, 18H). ^{13}C NMR (DMSO-d_6); δ = 158.0, 156.2, 155.4, 153.4, 152.8, 148.9, 149.0, 148.8, 145.8, 142.1, 139.2, 138.6, 137.9, 136.5, 132.6, 127.8, 127.6, 127.4, 127.0, 126.6, 125.9, 125.7, 125.4, 124.9, 124.7, 123.8, 123.5, 121.1, 116.5, 71.7, 34.1, 33.9, 31.6, and 31.0. MALDI-TOF-Ms Calculated for $C_{33}H_{27}N_9Ru$ ($[M]^+$) 649.14; found, 649.46. Anal. calcd for $C_{110}H_{106}N_{18}O_4Ru_2$: C, 67.88; H, 5.49; N, 12.95%. Found: 67.93; H, 5.99; N, 13.19%.

Sample preparation for Absorption and Emission Titrations

1 mM of the Ru_2L was prepared as a stock solution in CH_3CN solvent. The concentration of the solution was fixed at 10 μM [CH_3CN/10mM HEPES Buffer (pH = 7.4) (8/2, v/v)] for using absorption and emission measurements. 1mM stock solution of metal salts and anions were prepared, further, it is diluted to optimum concentration if lower molar concentration arises. Ten minutes stirring was required for Ru_2L with a metal ion, before monitoring the absorbance and emission titration experiment. In anion sensing, Ru_2L+Cu^{2+} with anions were stirred for two minutes prior to recording absorbance and emission titration experiment. For the emission spectrum, the excitation wavelength was fixed at 457 nm (such as Cu^{2+} ion added to Ru_2L and S^{2-} anion added to Ru_2L-Cu^{2+}).

Cell Culture

The human lung cancer cell line A549 was acquired from National Center for Cell Science (NCCS), Pune, India. The cells were cultured in F-12K medium (Sigma-Aldrich, USA), supplemented with 10% fetal bovine serum (Himedia, India) and 20 mL of penicillin/streptomycin as antibiotics (Himedia, India), in 96 well culture plates, at 37°C in a humidified atmosphere of 5% CO_2 in a CO_2 incubator (Thermo Scientific, USA) for 2-3 days earlier to monitoring experiment. All experiments were carried out using cells from passage 15 or less.

MTT assay

The cytotoxic activities of Ru_2L have been screened against the A549 human lung cancer cell lines by using MTT assay.[67] The stock solution of the Ru_2L was prepared by dissolving in dimethyl sulfoxide (DMSO) and then diluted separately with media to get different concentrations of working solution. Five thousand A549 cells per well were seeded which is treated with 200 μl of the Ru_2L and incubated for 24 hours. Washed three times with PBS buffer, 20 μl of MTT solution (5mg/mL in PBS) was added to each well and the plate was enfolded with aluminum foil and incubated for 4 h at 310 K. The purple colour formazan dye product was dissolved by addition of 100 μL of DMSO to each well. The optical density of absorbance was monitored at 570 nm using a 96-well microplate reader (Bio-Rad, Hercules, USA). Data were collected for three replicates each and used to calculate the respective mean. The percentage inhibition (PI) was calculated, from this data, using the formula

$$PI\ (\%) = [OD_{\text{untreated cells (control)}} - OD_{\text{treated cells}} / OD_{\text{untreated cells (control)}}] \times 100\%$$

From the values thus obtained, the IC_{50} values were monitored after 24 h treatment for A549 cells and were deduced from the curves obtained by plotting percentage inhibition against concentration.

Acridine orange (AO) and ethidium bromide (EB) staining

Apoptotic morphology was investigated by AO/EB double staining method as described by Spector et al. with some modifications.[68] Briefly, the cells were treated with IC_{50} concentration of the Ru_2L for 24 h. After incubation, the cells were harvested and washed with cold PBS. Cell pellets were re-suspended and diluted with PBS to a density of 5×10^5 cells/mL and mixed with 25 µL of AO/EB solution (3.8 µM of AO and 2.5 µM of EB in PBS) on clean microscope slide and immediately examined under fluorescent microscope (Carl Zeiss, Jena, Germany) with UV filter (450-490 nm). Three hundred cells for each sample were scored for viable, apoptotic or necrotic by staining the nucleus structure and membrane integrity and the percentage of apoptotic and necrotic cells were calculated accordingly.

Hoechst 33528 staining

A549 cells were cultured in separate six-well plates and incubated with 24 h at IC_{50} concentrations of Ru_2L. After incubation, the treated and control cells were gathered and stained with Hoechst 33258 stain (1 mg/mL, aqueous) for 5 min at room temperature.[69] A drop of cell suspension was placed on a glass slide, and a coverslip was laid over to reduce light diffraction. At random 300 cells (in triplicate) were observed in the fluorescent microscope fitted with a 355-377 nm filter, and the percentage of cells that reflected pathological changes was calculated. Data were collected for three replicates each and used to calculate the means and the standard deviations.

Cellular uptake study

Inherent fluorescence characteristics of Ru_2L were very much helpful to learn their internalization into the cells. A549 cells were seeded on a cover glass and allowed culture to adhere. Then, cells were treated with Ru_2L (10 µM) for 1 h. After incubation, the cells were washed with cold PBS immediately examined under a fluorescent microscope (Carl Zeiss, Jena, Germany) with UV filters (543-570 nm). Ru_2L was then incubated with two different concentration of Cu^{2+} (10 and 20 µM) for another 60 min. After two times washing with PBS, the Cu^{2+} loaded cells (Ru_2L-Cu^{2+}) were analysed by fluorescence imaging measurements. Further, Ru_2L-Cu^{2+} loaded cells were incubated for one hour with two different concentrations of sulfide anions (25 and 50 µM), then washed using PBS and captured the fluorescence images.

Conflicts of interest

There are no conflicts to declare.

Acknowledgements

The research was financially supported by the Department of Science and Technology, India under Water Technology Initiative scheme (DST/TM/WTI/2K16/258). MR thanks CSIR, New Delhi for a junior research fellowship.

References

1 S. J. Lippard, J. Berg, Principles of Bioinorganic Chemistry, University Science Books, Mill Valley, CA, 1994.
2 E. L. Que, D. W. Domaille, C. J. Chang, *Chem. Rev*., 2008, **108**, 1517.
3 D. G. J. Barceloux, D. Barceloux, *J. Clin. Toxicol*., 1999, **37**, 217.
4 P. Verwilst, K. Sunwoo, J. S. Kim, *Chem. Commun*., 2015, **51**, 5556.
5 World Health Organization, Environmental Health Criteria, World Health Organization, Geneva, 1981, No. 19.
6 L. R. Goodwin, D. Francom, F. P. Dieken, J. D. Taylor, M. W. Warenycia, R. J. Reiffenstein, G. Dowling, *J. Anal. Toxicol*., 1989, **13**, 105.
7 L. N. Osbern, R. O. Crapo, *Ann. Intern. Med*., 1981, **95**, 312.
8 R. J. Reiffenstein, W. C. Hulbert, S. H. Roth, *Annu. Rev. Pharmacol. Toxicol*., 1992, **32**, 109.
9 K. A. Brenneman, D. F. Meleason, M. Sar, M.W. Marshall, R. A. James, E. A. Gross, J. T. Martin, D. C. Dorman, *Toxicol. Pathol*., 2002, **30**, 200.
10 C. D. Gutsche, Calixarenes: An Introduction, Edition 2, RSC Publishing, 2008.
11 R. Joseph, C. P. Rao, *Chem. Rev*., 2011, **111**, 4658.
12 J. S. Kim, D. T. Quang, *Chem. Rev*., 2007, **107**, 3780.
13 H. J. Kim, M. H. Lee, L. Mutihac, J. Vicens, J. S. Kim, *Chem. Soc. Rev*., 2012, **41**, 1173.
14 Y. R. Kim, H. J. Seo, J. W. Oh, H. Lim, T. H. Kim, H. Kim, *Electroanalysis*, 2013, **25**, 1.
15 Z. Liu, W. He, Z. Guo, *Chem. Soc. Rev*., 2013, **42**, 1568.
16 A. Ghorai, J. Mondal, A. K. Manna, S. Chowdhury, G. K. Patra, *Anal. Methods*, 2018, **10**, 1063.
17 S. Radunz, H. R. Tschiche, D. Moldenhauer, U. R. Genger, *Sens. and Actuators B*, 2017, **251**, 490.
18 Q. Gao, W. Zhang, B. Song, R. Zhang, W. Guo, J. Yuan, *Anal. Chem.*, 2017, **89**, 4517.
19 D. R. Boer, L. Wu, P. Lincoln, M. Coll, *Angew. Chem. Int. Ed.*, 2014, **53**, 1949.
20 A. Notaro, G. Gasse, *Chem. Soc. Rev.*, 2017, **46**, 7317.
21 F. Heinemann, J. Karges, G. Gasser, *Acc. Chem. Res.*, 2017, **50**, 2727.
22 L. Tong, R. P. Thummel, *Chem. Sci.*, 2016, **7**, 6591.
23 I. Kostova, *Curr. Med. Chem*., 2006, **13**, 1085.
24 T. Ezaki, S. Nishiumi, T. Azuma, M. Yoshida, *Toxicol. Res.*, 2017, **6**, 843.
25 M. Groessl, E. Reisner, C. G Hartinger, R. Eichinger, O. Semenova, A. R. Timerbaev, M. A. Jakupec, V. B.Arion, B. K. Keppler, *J. Med. Chem*., 2007, **50**, 2185.
26 W. H. Ang, P. J. Dyson, *Eur. J. Inorg. Chem.*, 2006, **2006 (20)**, 4003.
27 Du, Y. Kang, Y. Zhao, W. Zheng, Y. Zhang, Y. Lin, Z. Wang, Y. Wang, Q. Luo, K. Wu, F. Wang, *Inorg. Chem.*, 2016, **55**, 4595.
28 B. J. Han, G. B. Jiang, J. Wang, W. Li, H. L. Huang, Y. J. Liu, *RSC Adv.*, 2014, **4**, 40899.
29 D. L. Ma, V. P. Y. Ma, D. S. H. Chan, K. H. Leung, H. Z. He, C. H. Leung, *Coord. Chem. Rev.*, 2012, **256**, 3087.
30 S. Khatua, M. Schmittel, *Org. Lett.*, 2013, **15**, 4422.
31 D. Saha, S. Das, S. Mardanya, S. Baitalik, *Dalton Trans.*, 2012, **41**, 8886.
32 P. A. Scattergood, P. I. P. Elliott, *Dalton Trans.*, 2017, **46**, 16343.

33 Z. Du, B. Song, W. Zhang, C. Duan, Y.L. Wang, C. Liu, R. Zhang, J. Yuan, *Angew. Chem. Int. Ed.*, 2018, **57**, 3999.
34 K. Samanta, D. S. Ranade, A. Upadhyay, P. P. Kulkarni, C. P. Rao, *ACS Appl. Mater. Interfaces,* 2017, **9**, 5109.
35 Y. Sun, J. Ma, D. Tian, H. Li, *Chem. Commun.*, 2016, **52**, 4602.
36 A. Nehra, D. S. Yarramala, C. P. Rao, *Chem. Eur. J.*, 2016, **22**, 8980.
37 J. Cho, T. Pradhan, Y. M. Lee, J. S. Kim, S. Kim, *Dalton Trans.*, 2014, **43**, 16178.
38 P. D. Beer, F. Szemes, P. Passaniti, M. Maestri, *Inorg. Chem.*, 2004, **43**, 3965.
39 S. Y. Park, J. H. Yoon, C. S. Hong, R. Souane, J. S. Kim, S. E. Matthews, J. Vicens, *J. Org. Chem.*, 2008, **73**, 8212.
40 V. Saravanan, A. Kannan, P. Rajakumar, *Sens. and Actuators B*, 2017, **242**, 904.
41 S. Rahman, Y. Assiri, A. N. Alodhayb, L. Y. Beaulieu, A. K. Oraby, P. E. Georghiou, *New J. Chem.*, 2016, **40**, 434.
42 X. Lou, D. Ou, Q. Li, Z. Li, *Chem. Commun.*, 2012, **48**, 8462.
43 R. Kaushik, A. Ghosh, D. A. Jose, *Coord. Chem. Rev*., 2017, **347**, 141.
44 M. Z. Zhang, H. H. Han, S. Z. Zhang, C. Y. Wang, Y. X. Lu, W. H. Zhu, *J. Mater. Chem. B*, 2017, **5**, 8780.
45 Shaily, A. Kumar, N. Ahmed, *Ind. Eng. Chem. Res.*, 2017, **56,** 6358.
46 M. Sun, H. Yu, H. Li, H. Xu, D. Huang, S. Wang, *Inorg. Chem.*, 2015, **54**, 3766.
47 F. Hou, L. Huang, P. Xi, J. Cheng, X. Zhao, G. Xie, Y. Shi, F. Cheng, X. Yao, D. Bai, Z. Zeng, *Inorg. Chem.*, 2012, **51**, 2454.
48 A. K. Mahapatra, S. Mondal, S. K. Manna, K. Maiti, R. Maji, M. R. Uddin, S. Mandal, D. Sarkar, T. K. Mondal, D. K. Mait, *Dalton Trans.*, 2015, **44**, 6490.
49 H. Li, *Anal. Chim. Acta.*, 2018, **1010**, 69.
50 J. Chen, Y. Li, W. Zhong, Q. Hou , H. Wang, X. Sun, P. Yi, *Sens. and Actuators B,* 2015, **206**, 230.
51 J. Chen, Y. Li , K. Lv , W. Zhong, H. Wang, Z. Wu, P. Yi, J. Jiang, *Sens. and Actuators B,* 2016, **224**, 298.
52 X. Yue, Z. Zhu, M. Zhang, Z. Ye, *Anal. Chem.*, 2015, **87**, 1839.
53 M. Li, Q. Liang, M. Zheng, C. Fang, S. Peng, M. Zhao, *Dalton Trans.*, 2013, **42**, 13509.
54 P. Zhang,Y. Wang,W. Huang, Z. Zhao, H. Li, H. Wang, C. He, J. Liu, Q. Zhang, *Sens. and Actuators B*, 2018, **255**, 283.
55 M. Bhatt, D. Maity, V. Hingu, E. Suresh, B. Ganguly, P. Paul, *New J. Chem.*, 2017, **41**, 12541.
56 R. Zhang, X. Yu, Y. Yin, Z. Ye, G. Wang, J. Yuan*, Anal. Chim. Acta.*, 2011, **691**, 83.
57 P. Zhang, L. Pei, Yu Chen, W. Xu, Q. Lin, J. Wang, J. Wu, Y. Shen, L. Ji, H. Chao, *Chem. Eur. J*., 2013, **19**, 15494.
58 N. Queyriaux, E. S. Andreiadis, S. Torelli, J. Pecaut, B. S. Veldkamp, E. A. Margulies, M. R. Wasielewski, M. C. Kerlidou, V. Artero, *Faraday Discuss.*, 2017, **198**, 251.
59 J. C. H. Acosta, M. A. Méndez, M. D. Scanlon, H. Vrubel, V. Amstutz, W. Adamiak, M. Opallo, H. H. Girault, *Chem. Sci.,* 2015, **6**, 1761.
60 W. Iali, P. H. Lanoe, S. Torelli, D. Jouvenot, F. Loiseau, C. Lebrun, O. Hamelin, S. Menage, *Angew. Chem. Int. Ed.,* 2015, **54**, 8415.
61 M. Q. Wang, K. Li, J. T. Hou, M. Y. Wu, Z. Huang, X. Q. Yu, *J. Org. Chem.,* 2012, **77**, 8350.
62 F. T. Andón, B. Fadeel, *Acc. Chem. Res.*, 2013, **46**, 733.
63 B. P. Sullivian, D. J. Salmon, T. J. Meyer, *Inorg. Chem.*, 1978, **17**, 3334.
64 V. V. S. Mummidivarapu, V. K. Hinge, K. Tabbasum, R. G. Gonnade, C. P. Rao, *J. Org. Chem*., 2013, **78**, 3570.
65 A. Baron, C. Herrero, A. Quaranta, M. F. Charlot, W. Leibl, B. Vauzeilles, A. Aukauloo, *Chem. Commun*., 2011, **47**, 11011.
66 B. S. Uppal, A. Zahid, P. I. P. Elliott, *Eur. J. Inorg. Chem*., 2013, 2571.
67 T. Mosmann, *J Immunol Methods*., 1983, **65**, 55.
68 D. L. Spector, R. D. Goldman, L. A. Leinwand, Cell: A Laboratory Manual, Culture and Biochemical Analysis of Cells, 1, Cold Spring Harbor Laboratory Press, Cold Spring Harbor, New York, 1998, p. 34.1.
69 G. P. A. H. Kasibhatla, D. Finucane, T. Brunner, E. B. Wetzel, D. R. Green, Protocol: Staining of suspension cells with Hoechst 33258 to detect apoptosis. Cell: A Laboratory Manual Culture and Biochemical Analysis of Cells; Vol. 1, CSHL press, USA, 1998, p. 15.5.

ART**Table of Contents entry** ame

The supramolecular sensor Ru_2L was designed by joining bis-ruthenium (II) polypyridyl complex with p-tert-butyl calix[4]arene platform through a 1,2,3-triazole linker and used for sensing of copper (II) and sulphide ions by fluorescence.

View Article Online
DOI: 10.1039/C9NJ01632E